Published online 02 September 2014 *Nucleic Acids Research, 2014, Vol. 42, No. 17* ***10927–10942***
doi: 10.1093/nar/gku755

Arabidopsis SEPALLATA proteins differ in cooperative DNA-binding during the formation of floral quartet-like complexes

Khushboo Jetha[1], Günter Theißen[1] and Rainer Melzer[1,2,*]

[1]Department of Genetics, Friedrich Schiller University Jena, Philosophenweg 12, D-07743 Jena, Germany and
[2]Department of Genetics, Institute of Biology, University of Leipzig, Talstraße 33, D-04103 Leipzig, Germany

Received March 13, 2014; Revised August 05, 2014; Accepted August 6, 2014

ABSTRACT

The *SEPALLATA* (*SEP*) genes of *Arabidopsis thaliana* encode MADS-domain transcription factors that specify the identity of all floral organs. The four *Arabidopsis SEP* genes function in a largely yet not completely redundant manner. Here, we analysed interactions of the SEP proteins with DNA. All of the proteins were capable of forming tetrameric quartet-like complexes on DNA fragments carrying two sequence elements termed CArG-boxes. Distances between the CArG-boxes for strong cooperative DNA-binding were in the range of 4–6 helical turns. However, SEP1 also bound strongly to CArG-box pairs separated by smaller or larger distances, whereas SEP2 preferred large and SEP4 preferred small intersite distances for binding. Cooperative binding of SEP3 was comparatively weak for most of the intersite distances tested. All SEP proteins constituted floral quartet-like complexes together with the floral homeotic proteins APETALA3 (AP3) and PISTILLATA (PI) on the target genes *AP3* and *SEP3*. Our results suggest an important part of an explanation for why the different SEP proteins have largely, but not completely redundant functions in determining floral organ identity: they may bind to largely overlapping, but not identical sets of target genes that differ in the arrangement and spacing of the CArG-boxes in their *cis*-regulatory regions.

INTRODUCTION

SEPALLATA (SEP)-like MADS-domain transcription factors constitute a subfamily of homeotic proteins that regulate a plethora of processes during flower development, ranging from floral meristem specification to floral organ and ovule identity determination (1). The *Arabidopsis thaliana* genome contains four *SEP* genes, termed *SEP1*, *SEP2*, *SEP3* and *SEP4*, formerly known as *AGL2*, *AGL4*, *AGL9* and *AGL3*, respectively (2,3). In *sep1 sep2 sep3* triple mutants, primorida that normally develop into petals, stamens and carpels develop into sepal-like organs (2). Also the determinacy of floral growth is disturbed in *sep1 sep2 sep3* triple mutants, and floral organs are continuously produced inside of the fourth floral whorl (2). This drastic mutant phenotype is not seen in the single mutants and the genes have therefore been considered to be largely redundant (2). The severity of the mutant phenotype is further increased if all four *SEP* genes are mutated. *sep1 sep2 sep3 sep4* quadruple mutants develop flower-like structures possessing only leaf-like organs instead of the sepals observed in *sep1 sep2 sep3* flowers (3). Analysis of further mutant combinations revealed that *SEP4* is not only involved in specifying sepal identity but also contributes to the specification of the other floral organs (3). The picture emerging from this data set is that *SEP* genes determine floral organ identity in an additive yet largely redundant manner (3). Phylogenetic analyses indicate that a basal duplication leading to a clade containing *SEP1*, *SEP2* and *SEP4* and a second clade containing *SEP3* occurred prior to the origin of the lineage that led to the extant angiosperms (4). *SEP1/2/4*- and *SEP3*-like genes thus coexisted for many millions of years and remained highly conserved throughout angiosperm evolution, indicating that there is some selective advantage of keeping several copies of *SEP*-like genes (5). Genetic evidence that *SEP1, SEP2* and *SEP3* are not completely redundant to *SEP4* is already provided by the different phenotypes of the triple compared to the quadruple mutants described above. Furthermore, *SEP4* has a more prominent role in determining meristem identity as compared to that of the other *SEP* genes, because double mutants of *SEP4* and the floral homeotic gene *APETALA1* (*AP1*) display a cauliflower-like mutant phenotype which is observed neither in the single mutants nor when other *sep* mutants are combined with *ap1* (3). Redundancy among *SEP1*, *SEP2* and *SEP3* is not complete either. For example, *sep3* single mutants have phenotypes that resemble intermediate *ap1* mutant alleles, with petals that develop sepa-

*To whom correspondence should be addressed. Tel: +49 3641 949564; Fax: +49 3641 949552; Email: rainer.melzer@uni-jena.de

loid characteristics (6). Also, double mutants in which the *sep3–2* mutant allele is combined with the weak *lfy-2* allele possess dramatic floral defects that are not observed in either of the single mutants (7). This indicates that the other *SEP* genes cannot compensate for the mutated *sep3* allele when *lfy* is also mutated.

Taken together, these data raise the question of how the similarities and differences among the different *SEP* genes are caused by molecular interactions. At least two (not mutually exclusive) explanations may be considered: The functional differences between the various *SEP* genes may be caused by differences in expression patterns, expression levels or stabilities of the *SEP* mRNAs or proteins. Alternatively, different *SEP* genes were retained because the proteins they encode have inherently different biochemical or biophysical properties. Concerning the first possibility, differences in the expression pattern among the four *SEP* genes are indeed well documented (3,8–11). For example, *SEP1*, *SEP2* and *SEP4* are expressed throughout the floral meristem and in the sepal primorida very early during flower development. In contrast, *SEP3* is expressed in the floral meristem but not in the sepal primordia (3,8,10–11). Unlike the other *SEP* genes, the expression of *SEP4* is not confined to the flower but also detected in leaves and floral stems (9). It is very likely that these differences in expression pattern also relate to different functions of the *SEP* genes (5). However, while variations in transcript stability, expression strength and pattern may contribute to differential functions of the *SEP* genes, there are several lines of evidence indicating that diversification of the biophysical and biochemical properties of SEP proteins have occurred, too. For example, SEP3 has a stronger transcription activation potential than SEP1 and SEP2 (12). Also, the interaction partners of the different SEP proteins differ (13–15). Intriguingly, in a large scale yeast two-hybrid screen, there was only a single MADS-domain protein detected with which all SEP proteins could interact, namely, SUPPRESSOR OF OVEREXPRESSION OF CONSTANS1 (SOC1) (13).

While the transcription activation ability and protein–protein interactions of SEP proteins have been studied in some detail (12–15), one of the most critical determinants of transcription factor function, i.e. its interaction with DNA, has gained relatively little attention so far. It is known for SEP1, SEP3 and SEP4 that they bind as homodimers to DNA-elements termed CArG-boxes (for CCArichGG; consensus 5′-CC(A/T)$_6$GG-3′) (16–17,18). However, another important aspect of SEP protein function is that they likely constitute tetrameric DNA-bound complexes to govern flower development. The formation of these floral quartet-like complexes is of special interest as they have been proposed to assemble cooperatively on DNA (5,19). When DNA-binding is cooperative, small increments in protein concentration can lead to drastic changes in target gene occupancy, essentially resulting in a switch-like regulation of target genes (20). SEP proteins are involved in sharp developmental transitions like the ones that occur during the initiation of flowering and the specification of floral organs, which may require such a switch-like regulation of target genes (20). We previously presented evidence indicating that SEP3 forms tetrameric complexes that bind cooperatively to DNA fragments carrying appropriately spaced CArG-boxes (18). Furthermore, we provided evidence indicating that SEP3 is able to constitute a DNA-binding heterotetramer with APETALA3 (AP3) and PISTILLATA (PI), two MADS-domain proteins essential for petal and stamen formation (21). However, whether the other SEP proteins can assemble cooperatively on DNA as homo- and heterotetrameric complexes and to which extent DNA-binding differs among the individual SEP proteins remained unknown. Also, knowledge about differential cooperative DNA-binding on *bona fide* target genes remains scarce.

Using electrophoretic mobility shift assays (EMSAs) we show here that the four SEP proteins from *Arabidopsis* possess the ability to bind cooperatively to DNA as tetramers. For all SEP proteins, cooperative DNA-binding was strongest for a relatively short distance of 4–6 helical turns between the CArG-boxes. However, differences in the degree of cooperative binding as well as in the preferred distances between the CArG-boxes were detected. Differences were also detected in the binding of SEP protein complexes to genuine target gene promoters. Thus, the high functional similarities as well as the subtle differences among the *SEP* genes are reflected at the level of cooperative DNA-binding of the SEP proteins. This could be one of the molecular mechanisms explaining how both redundant and distinct functions of the SEP proteins are established.

MATERIALS AND METHODS

Cloning of the SEP cDNAs into pTNT vector

Full-length coding regions of all *SEP* cDNAs were cloned into pTNT for *in vitro* translation. The *SEP3* construct used in this study has been described previously (18). *SEP1* (gi. 145358077), *SEP2* (gi. 42563430) and *SEP4* (gi. 145359878) were amplified from a cDNA pool and cloned into pTNT using XhoI/SalI (*SEP1* and *SEP2*) and XbaI/XhoI (*SEP4*) recognition sites. AP3 and PI constructs used have been described previously (22). Primers used for cloning are listed in Supplementary Table S1.

Design of DNA probes

A CArG-box was defined as a sequence having the consensus 5′-CC(A/T)$_6$GG-3′. A maximum of two mismatches to this sequence were allowed. However, these mismatches were not permitted to introduce a G at the two positions occupied by a C in the consensus or a C at the two positions occupied by a G in the consensus. In addition, the mismatches were not allowed to totally eliminate the CC or GG nucleotides flanking the A/T-rich core.

DNA probes containing only one CArG-box and those containing two CArG-boxes spaced by 6–9 helical turns have been described previously (18,21). For all other DNA probes, corresponding single stranded oligonucleotides were annealed. After annealing, the double stranded fragments were cloned into pBluescript SK II+ using an EcoRI restriction site or into pJET1.2. For EMSA analysis, DNA fragments were excised from the plasmid and gel purified. The oligonucleotide employed in saturation binding assays was used directly after annealing without cloning into a vector and gel purification.

DNA fragments were labelled radioactively using either the Klenow fragment (exo-) and [α-^{32}P] dATP, or T4 polynucleotide kinase and [γ-^{32}P] ATP. Labelled probes were purified using the illustra ProbeQuant kit (GE healthcare). The labelled probes were stored at −20°C.

Sequences of the probes used are listed in Supplementary Table S2.

In vitro transcription/translation and EMSAs

In vitro transcription/translation was done using the SP6 QuickCoupled Transcription/Translation mix (Promega) according to the manufacturer's instructions. Freshly translated proteins were used directly. Only in exceptional cases the protein solution was shock frozen in liquid nitrogen and stored at −80°C until later use. The composition of the protein-DNA binding reaction was essentially as described previously (18) except that the concentration of competitor DNA was 386 ng per reaction. The competitor DNA used in the binding buffer was poly(dI-dC) for the assays involving probes from the regulatory regions of the *AP3* and *SEP3* gene and herring sperm DNA for all other assays. The concentration of probe used was ≈0.015 nM. The volume of the *in vitro* translated protein solution used for a single binding reaction varied between 0.1 and 5 μl (when 0.1 or 0.5 μl protein was used, it was diluted tenfold with bovine serum albumin (10 mg/ml in water) for ease of pipetting).

The reaction was incubated on ice for several hours to overnight for the DNA and protein to interact. The reaction mix was then loaded onto a native 5% polyacrylamide gel with 0.5× TBE running buffer. Gel run was performed at room temperature at 7.5 V/cm for 150–200 min. Afterwards, the gel was dried and exposed onto a phosphorimager screen. Phosphorimager screens were scanned using the FLA 7000 (Fujifilm). The images were analysed using Multi Gauge (Fujifilm).

In EMSAs, SEP4 behaved differently from the other SEP proteins in that binding was always relatively weak. During later stages of the project (i.e. when saturation binding assays and the analyses of binding to putative direct targets were conducted) we were not able to reliably obtain detectable DNA-binding of SEP4, the reasons for which are not entirely clear. However, it seems as though different batches of the *in vitro* translation mixture yielded very different amounts of active (i.e. DNA-binding) SEP4 protein. Very likely, batches used in later stages of the project were not suitable for producing sufficient amounts of active SEP4 protein. Though this is a suboptimal situation, too low concentration of functional protein in certain *in vitro* translation reactions do not hinder conclusions on SEP4 binding specificity in experiments where protein-DNA complexes were detected and hence the respective data were taken into account for the analyses.

Calculation of k_{coop} ratios

The ratio of two macroscopic association constants K_a and K_b for protein dimers binding to two different DNA probes *a* and *b* that each carry two binding sites can be expressed as

$$\frac{K_a}{K_b} = \frac{Y_{P_2D_a}}{[P_a]^2 \cdot Y_{D_a}} \cdot \frac{[P_b]^2 \cdot Y_{D_b}}{Y_{P_2D_b}} \quad (1)$$

similar to what has been described previously (23). Y_{D_a} and Y_{D_b} represent the fraction of free DNA for probe *a* and *b*, respectively, and $Y_{P_2D_a}$ and $Y_{P_2D_b}$ represent the fraction of the respective DNA probes that are bound by two protein dimers. $[P_a]$ and $[P_b]$ are the concentrations of free protein dimers in each of the reactions. Here and in the subsequent equations we assume that in the absence of DNA the protein is present predominantly in dimeric form. This is a necessary simplification as the dissociation constant for dimerization is unknown. However, previous data indicate that most of the protein indeed exists in dimeric form in solution at the concentrations used, as binding curves based on this assumption fitted well to the experimental data (18). Also in the present work, binding curves generated under this assumption were in good agreement with the original data.

For a probe carrying two CArG-boxes, the macroscopic association constant K_a (or K_b) for the simultaneous binding of two dimers can be expressed as the product of the microscopic association constants

$$K_a = k_{a1}k_{a2}k_{\text{coop}} \quad (2)$$

where k_{a1} is the microscopic association constant for binding of the first protein dimer and k_{a2} the microscopic association constant for binding of the second dimer to DNA. k_{coop} is the constant describing cooperative interactions (24). For the experiments analysed, DNA-probes carrying two identical CArG-boxes were used. Thus, k_{a1} should equal k_{a2} and Equation (2) simplifies to

$$K_a = k_{a1}^2 k_{\text{coop}} \quad (3)$$

(24). Combining Equations (1) and (3), the ratio of the two macroscopic association constants can then be expressed as

$$\frac{K_a}{K_b} = \frac{k_{a1}^2 k_{\text{coop}a}}{k_{b1}^2 k_{\text{coop}b}} \quad (4)$$

As only the affinities to DNA probes carrying identical CArG-boxes are compared, k_{a1} should equal k_{b1}. Thus, Equation (4) simplifies to

$$\frac{K_a}{K_b} = \frac{k_{\text{coop}a}}{k_{\text{coop}b}} \quad (5)$$

Combining Equations (1) and (5) yields

$$\frac{k_{\text{coop}a}}{k_{\text{coop}b}} = \frac{Y_{P_2D_a}}{[P_a]^2 \cdot Y_{D_a}} \cdot \frac{[P_b]^2 \cdot Y_{D_b}}{Y_{P_2D_b}} \quad (6)$$

As the proteins are produced by *in vitro* translation, the total protein concentration, and hence also the concentration of free protein dimers ($[P_a]$ and $[P_b]$), remain unknown in our assays. However, for

$$\sqrt{K_a} \cdot [D_s] < 0.14 \quad (7)$$

with $[D_s]$ being the total concentration of DNA sites, the fraction of protein bound to the DNA is negligible and thus the total protein concentration $[P_t]$ is very close to the concentration of free protein, essentially as described (25). In

our experiments, we kept the total DNA site concentration below 0.03 nM (equalling two times the probe concentration of 0.015 nM, as probes carry two binding sites). Furthermore, saturation binding assays showed that the equilibrium affinity constant of individual SEP dimers to DNA is around $60{\cdot}10^6$ M^{-1} for SEP1 and SEP2 and around $150{\cdot}10^6$ M^{-1} for SEP3 (see below). Taking this into account and inserting K_a as given by Equation (3) into Equation (7) approximately yields $k_{coop} < 6000$ for SEP1 and SEP2 and $k_{coop} < 950$ for SEP3. If these conditions are fulfilled and if protein aliquots from the same *in vitro* translation are used to determine k_{coop} ratios, then $[P_a] \approx [P_t] \approx [P_b]$ and hence Equation (6) simplifies to

$$\frac{k_{coopa}}{k_{coopb}} = \frac{Y_{P_2D_a} \cdot Y_{D_b}}{Y_{D_a} \cdot Y_{P_2D_b}} \tag{8}$$

k_{coop} ratios exceeding 950 and 6000 cannot be determined using Equation (8). However, such high ratios would also imply large differences in probe saturation that were anyway difficult to quantify reliably and therefore were not taken into account for the analysis (Figure 2).

Determination of cooperativity constants

Beyond determining k_{coop} ratios (see above), apparent k_{coop} values were determined in EMSAs in which increasing concentrations of *in vitro* translated protein were added to a constant amount of DNA probe. k_{coop} was inferred using equations previously described (24) using GraphPad Prism 5. The SEP protein concentrations were not known in our assays. However, using the volume of the *in vitro* translation mixture as a proxy for the SEP protein dimer concentration, we inferred apparent k_{coop} values essentially as previously described (18). The detection of single dimers bound to DNA is of critical importance for inferring k_{coop} values (25). In our experimental setup, k_{coop} values appeared to vary considerably when fractional saturation of single dimers bound to DNA was below 0.065 in all lanes analysed for a specific experiment. Using equations described previously (26) it follows that a k_{coop} value of ≈200 is the upper limit that can be determined by our assay.

Saturation binding assay

To determine the DNA-binding affinity of the SEP proteins as dimers, a short DNA probe harbouring a consensus CArG-box sequence from the regulatory intron of *AGAMOUS* (*AG*) was used in EMSAs. In these assays, a constant amount of the SEP protein (provided by 2–4 μl of the *in vitro* translation solution containing the protein) was titrated against increasing concentrations of DNA (1.05, 2.25, 4.50, 9.00, 18.00, 36.23, 72.45, 108.60 and 144.90 nM in each reaction, respectively), similar to what has been described (22,27–28).

Briefly, the apparent equilibrium association constant for a protein dimer binding to naked DNA is

$$K_{\dim N} = \frac{[PD]}{[P] \cdot [D]} \tag{9}$$

with $[PD]$, $[P]$ and $[D]$ being the concentration of the protein-DNA-complex, free protein and free DNA, respectively.

The concentration of free protein can be expressed as

$$[P] = [P_t] - [PD], \tag{10}$$

where $[P_t]$ is the total concentration of protein dimers that are capable of DNA binding (excluding aberrant, e.g. misfolded, proteins that cannot bind DNA).

Substituting $[P]$ by $[P_t] - [PD]$ in Equation (9) yields

$$K_{\dim N} = \frac{[PD]}{([P_t] - [PD]) \cdot [D]} \tag{11}$$

Rearrangement yields

$$[PD] = \frac{[P_t] \cdot [D]}{\frac{1}{K_{\dim N}} + [D]} \tag{12}$$

Plotting $[PD]$ versus $[D]$ enables the determination of $[P_t]$ and $K_{\dim N}$ using a non-linear regression analysis with Equation (12) and GraphPad Prism 5.

The rational of this experimental design is that DNA concentration is increased in a stepwise fashion to a value at which protein-DNA-complexes do not increase in concentration anymore. At these DNA concentrations virtually all functional protein is bound by DNA. As the DNA concentration used is known, inferences about the concentration of the protein-DNA complex and hence about the concentration of functional protein, i.e. $[P_t]$ and about $K_{\dim N}$ can be made.

The Gibbs energy $\Delta G_{\dim N}$ for the binding of a SEP dimer to naked DNA was determined using the equation

$$\Delta G_{\dim N} = -RT \ln K_{\dim N} \tag{13}$$

with R being the gas constant ($8.314 \cdot 10^{-3}$ kJ/(K·mol)) and T the absolute temperature (274.15 K; corresponding to 1°C, the temperature at which the protein-DNA reaction was incubated).

Calculations of protein concentrations necessary for half-occupancy of DNA

Fractional saturation in a system where two DNA-binding sites can be occupied by a protein ligand can be determined using previously described equations (24). Considering a system with two identical neighbouring CArG-boxes, the fractional saturation $Y_{P_2D_N}$ for two dimers bound simultaneously to naked DNA is

$$Y_{P_2D_N} = \frac{K_{\dim N} \cdot K_{\dim N} \cdot k_{coop} \cdot [P]^2}{1 + (K_{\dim N} + K_{\dim N}) \cdot [P] + K_{\dim N} \cdot K_{\dim N} \cdot k_{coop} \cdot [P]^2} \tag{14}$$

Half-occupation is defined here to be achieved when $Y_{P_2D_N} = 0.5$; i.e. when 50% of the DNA fragments are bound by two protein dimers. We used transition curves based on Equation (14) to infer the protein dimer concentration $[P]$ at which half-occupation is achieved.

To calculate the half saturation of DNA in which one CArG-box is covered by histones, we first inferred the Gibbs

energy $\Delta G_{\mathrm{dim}\,H}$ for binding of a single protein dimer to the CArG-box covered by histones using the equation

$$\Delta G_{\mathrm{dim}\,H} = \Delta G_{\mathrm{dim}\,N} + \Delta G_P \quad (15)$$

where ΔG_P is the energy cost (or penalty) of breaking a set of histone-DNA contacts and thereby exposing the dimer binding site which is covered by histones. The equilibrium association constant for binding of a single dimer to nucleosomal DNA can in turn be determined using the equation

$$K_{\mathrm{dim}\,H} = e^{-\Delta G_H / RT} \quad (16)$$

$K_{\mathrm{dim}\,H}$ can then be inserted in Equation (14) to determine the fractional saturation $Y_{P_2D_H}$ for two dimers bound simultaneously to DNA on which one of the two CArG-boxes is covered by histones:

$$Y_{P_2D_H} = \frac{K_{\mathrm{dim}\,N} \cdot K_{\mathrm{dim}\,H} \cdot k_{\mathrm{coop}} \cdot [P]^2}{1+(K_{\mathrm{dim}\,N}+K_{\mathrm{dim}\,H}) \cdot [P]+K_{\mathrm{dim}\,N} \cdot K_{\mathrm{dim}\,H} \cdot k_{\mathrm{coop}} \cdot [P]^2} \quad (17)$$

The protein dimer concentration $[P]$ necessary for half-occupation was determined using transition curves as described above for naked DNA.

RESULTS

All *Arabidopsis* SEPALLATA proteins cooperatively form homotetrameric quartet-like complexes *in vitro*

It had previously been shown that SEP3 has the ability to bind as a homodimer to a DNA fragment carrying a single CArG-box and that four SEP3 proteins bind to a DNA probe carrying two CArG-boxes (18). The different complexes can be identified by EMSAs based on their characteristic gel electrophoretic mobilities (18). To determine whether SEP1, SEP2 and SEP4 bind to DNA with the same stoichiometry as SEP3, EMSAs using DNA probes carrying one and two CArG-boxes were performed. The CArG-box sequence was derived from the regulatory intron of *AG*. In these EMSAs, SEP1, SEP2 and SEP4 formed protein-DNA complexes with electrophoretic mobilities very similar to the respective SEP3-DNA complexes (Figure 1). This indicates that all four SEP proteins bind as homodimers to DNA fragments carrying one CArG-box (Figure 1, compare lanes 2, 6 and 14 with lane 10) and that two SEP-dimers bind to DNA fragments carrying two CArG-boxes (Figure 1, compare lanes 1, 5 and 13 with lane 9).

We have also previously provided evidence that SEP3 binds to DNA probes carrying two CArG-boxes separated by 6–9 helical turns by forming a homotetramer and looping the DNA between the binding sites (18). To investigate whether SEP3 can accommodate binding to CArG-boxes separated by distances smaller than 6 helical turns and whether also SEP1, SEP2 and SEP4 are capable of forming homotetrameric complexes and looping the DNA, a series of DNA-probes having two identical CArG-boxes (the CArG-box sequence was derived from the regulatory intron of *AG*) separated by 1–9 helical turns in steps of half-helical turns each (assuming 10.5 bp/turn), were employed. If tetramer formation occurs, it would be expected to be stronger when the CArG-boxes are separated by an integral number of helical turns than when the spacing is non-integral, as previously described (18).

Our analyses indicated that for all four SEP proteins, two dimers bound relatively strongly to CArG-boxes separated by 5 helical turns (Figure 2). However, binding strength of two SEP-dimers to DNA decreased when a probe with CArG-boxes spaced by 5.5 helical turns was used and increased again when the distance between the binding sites was 6 helical turns (Figure 2, compare lanes 10–12 in A and B, lanes 11–13 in C and D; see Figure 2E–H for a quantitative evaluation). This stereo-specific pattern of strong and weak binding to CArG-boxes separated by integral and half-integral numbers of helical turns was observed for SEP1, SEP2 and SEP4 over the entire range of CArG-box distances for which binding could be detected (Figure 2). For SEP3 the periodicity in binding was only observed for CArG-boxes separated by 4 or more helical turns, whereas the signal corresponding to 2 dimers bound to DNA increased for CArG-boxes spaced between 2 and 4 helical turns without showing a periodic pattern of strong and weak binding (Figure 2G). Besides a periodic increase and

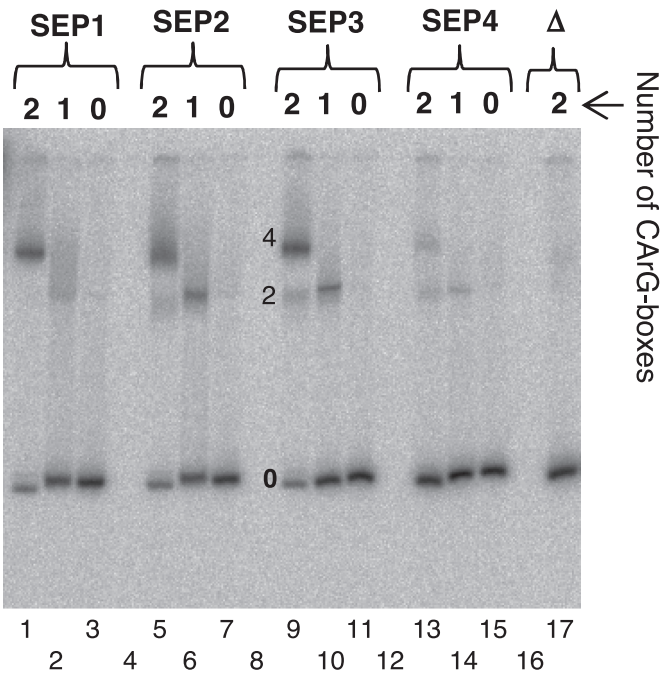

Figure 1. Binding of the SEP proteins to CArG-boxes. Above the gel, 0, 1 and 2 denotes the number of CArG-boxes present on the different probes. On the probe containing two CArG-boxes, these were separated by 6 helical turns. DNA probes were ≈150 bp long. The proteins applied are noted above the gel. Bands labelled '4' '2' and '0' represent the respective number of protein molecules bound. Δ represents a negative control in which the *in vitro* translation assay was programmed with a pTNT vector not containing a cDNA insert and incubated with the probe containing two CArG-boxes. The numbers below the gel picture denote lane numbers, with 4, 8, 12 and 16 representing empty lanes.The volumes of *in vitro* translated protein solution used for the binding reactions were: 1 μl in lanes 1 and 9; 1.5 μl each in lanes 10 and 11; 2 μl each in lanes 5 and 13; 3 μl each in 14 and 15; 4 μl each in lanes 2 and 3; 5 μl each in lanes 6, 7 and 17 (different volumes were chosen to detect the different protein-DNA complexes easily).

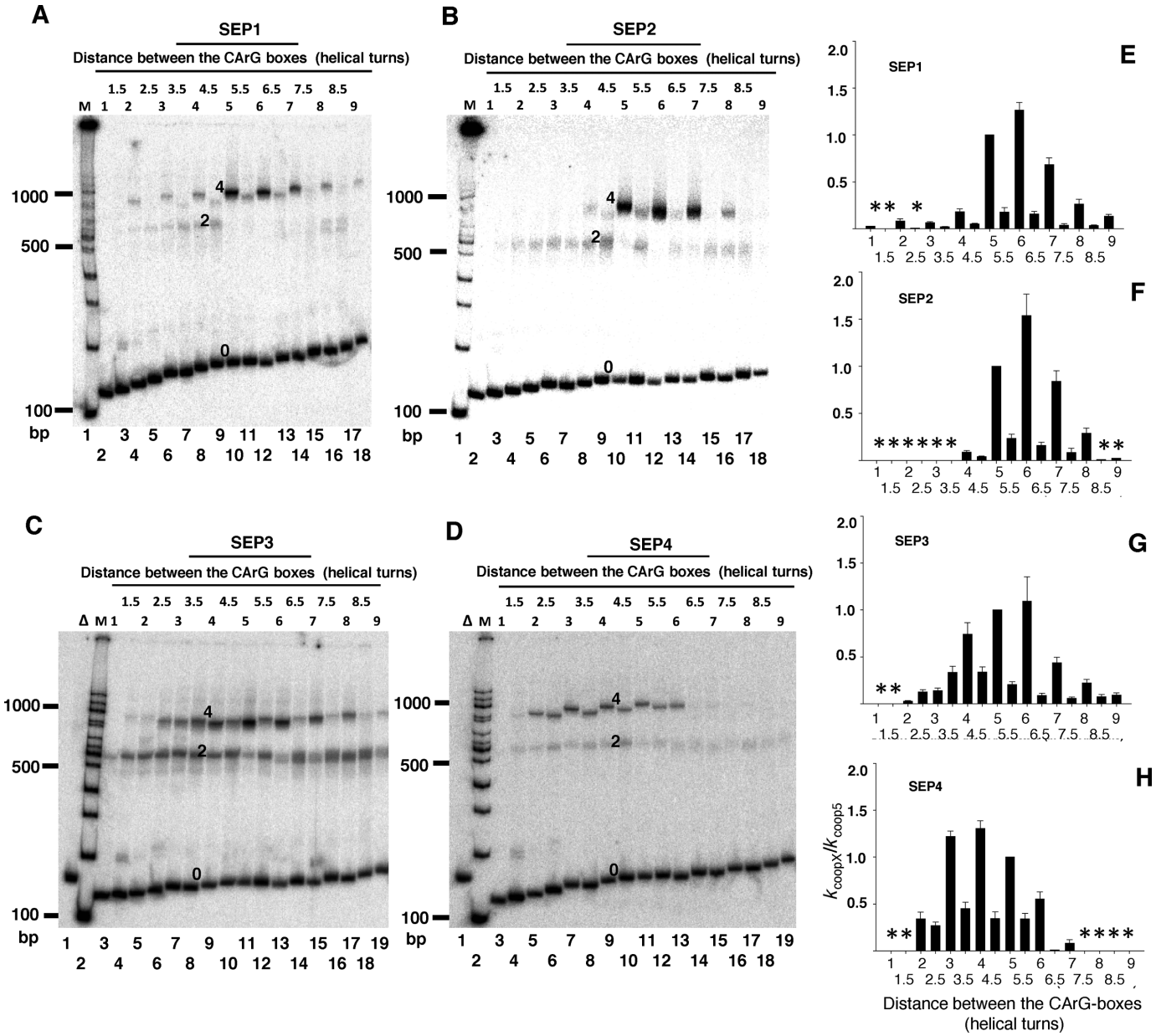

Figure 2. Stereo-specific DNA-binding and tetrameric complex formation by the four SEP proteins. DNA probes with two identical CArG-boxes spaced by 1–9 helical turns, as noted above the gel were used. Labelled DNA probes were incubated together with 0.2 μl *in vitro* translated SEP1 solution (A), 1.5 μl SEP2 solution (B), 0.2 μl SEP3 solution (C) and 1 μl SEP4 solution (D), respectively. E–H. Quantitative analysis of stereo-specific DNA-binding by the four SEP proteins. Ratios of cooperativity constants are plotted for each DNA probe taking the cooperativity constant of the probe with CArG-boxes spaced by 5 helical turns as a reference. Error bars represents the standard error of the mean ($n = 3$ to 6). Asterisks indicate probes with which a complex of two protein dimers bound to DNA was either never or only once detected. Lane and band labelling is analogous to Figure 1. M denotes the marker lane in which a radioactively labelled DNA ladder (100 bp ladder, NEB) was applied. The electrophoretic mobility of complexes composed of four proteins and DNA varied slightly depending on the DNA probe used (compare lanes 8, 9 and 10 in Figure 2D, for example). This can very likely be attributed to the ability of MADS-domain proteins to bend DNA (18,22). If two MADS-domain protein dimers bind on the same face of the DNA-helix, bending angles add up and the protein-DNA complex migrates relatively slowly through the gel. The formation of a looped complex would further reduce the electrophoretic mobility. In contrast, if dimers bind on opposite sides of the helix, the bends counteract each other and the protein-DNA complex can migrate relatively fast through the gel.

Table 1. Equilibrium affinity constants of SEP proteins binding to a single CArG-box

Protein	$K_{\mathrm{dim}\,N}$ ($\cdot 10^6$ M^{-1})	Gibbs energy (kJ/mol)
SEP1	52 ± 7	-40.5
SEP2	68 ± 22	-41.1
SEP3	150 ± 30	-42.9

decrease in binding affinity of the SEP proteins, we also observed that the binding strength of two SEP-dimers to DNA was dependent on the distance between the CArG-boxes. To compare differences in binding of the individual proteins to the different DNA probes, relative cooperativity constants were calculated using Equation (8). Binding to a probe in which CArG-boxes were separated by 5 helical turns was used as a reference here (Figure 2E–H). These analyses showed that SEP1, SEP2 and SEP3 bound most strongly to DNA probes having CArG-boxes separated by 6 helical turns; whereas SEP4 showed maximum binding when the CArG-boxes were separated by 4 helical turns (Figure 2E–H).

In general, SEP1 and SEP3 constituted complexes composed of four proteins bound to DNA over a wide range of CArG-box distances from 2 to 9 helical turns. In contrast, binding of SEP2 to CArG-boxes separated by less than 4 helical turns was barely detectable at the protein concentrations used. Yet another binding pattern was observed for SEP4, which preferred binding to CArG-boxes separated by small distances and showed only very weak binding for CArG-boxes separated by more than 6 helical turns.

For none of the SEP proteins could we reproducibly detect binding of four proteins to CArG-boxes separated by 1 or 1.5 helical turns, although very faint signals were occasionally observed (Figure 2).

The above described analyses indicated that all SEP proteins bind cooperatively to DNA probes with suitably separated CArG-boxes. To further substantiate these findings we extended our analyses beyond the determination of relative cooperativity constants and attempted to determine apparent k_{coop} values. k_{coop} is a constant describing cooperativity of binding of two SEP dimers to two CArG-boxes on the same DNA fragment. k_{coop} values of 1 indicate that binding is not cooperative whereas values above 1 are indicative of cooperativity in binding (24). Determination of k_{coop} also allowed estimating differences in the degree of cooperative binding among the SEP proteins. Binding of all four SEP proteins to DNA-probes having a pair of CArG-boxes separated by 2, 6 and 9 helical turns (Figure 3) was analysed.

All four SEP proteins bound with strong cooperativity to CArG-boxes separated by 6 helical turns (Figure 3), as is indicated by the low amount of singly bound dimers seen in all gels. The k_{coop} value determined for SEP3 binding to this probe was slightly lower than previously estimated (18), possibly owing to difficulties to precisely determine relatively high k_{coop} values. For SEP1, cooperativity was also high for CArG-boxes separated by 2 and 9 helical turns (Figure 3A). However, while for a probe in which CArG-boxes were spaced by 6 helical turns a tetrameric signal was readily detected with the lowest protein concentration used, this was not the case for DNA-probes in which CArG-boxes were spaced by 2 or 9 helical turns (Figure 3A, compare lanes 2, 8, 14), indicating that cooperativity was strongest for the probe with CArG-boxes separated by 6 turns. In comparison to SEP1, SEP3 appeared to bind with slightly lower cooperativity to CArG-boxes separated by 6 helical turns and with much weaker cooperativity to CArG-box pairs separated by 2 and 9 turns (Figure 3C). For SEP2, formation of potential tetrameric protein-DNA complexes was observed only at relatively high protein concentrations for CArG-boxes separated by 2 and 9 helical turns, indicating that cooperative binding is much lower here, as compared to the probe with CArG-boxes spaced by 6 helical turns (Figure 3B). However, tetrameric complexes were observed at relatively high protein concentrations for CArG-boxes separated by 9 turns but not or only weaker with CArG-boxes separated by 2 helical turns, indicating that cooperative binding is relatively stronger with CArG-boxes separated by 9 helical turns (Figure 3B). SEP4 behaved inverse to SEP2, with relatively strong binding to CArG-boxes spaced by 2 helical turns and very weak binding to CArG-boxes separated by 9 helical turns (Figure 3D). Overall, the data obtained from these cooperative binding analyses are consistent with the results of the stereo-specific binding assay described above.

SEP dimers bind with different affinities to DNA

As differences in cooperative DNA-binding were observed among the SEP proteins, we were interested to know if the binding affinity of individual dimers to DNA also differed. For this purpose, saturation-binding assays were carried out in which a constant amount of SEP protein was titrated against increasing amounts of a DNA probe carrying a single CArG-box. The CArG-box used possessed the same sequence as the one in the previous experiments. The apparent association constant K_{dimN} was slightly higher for SEP3 than for SEP1 and SEP2 (Table 1, Supplementary Figure S1), indicating that also at the level of individual dimers binding to DNA, affinity differences among the SEP proteins may exist. For SEP4, binding to the single CArG-box was very weak or undetectable and therefore we were not able to determine an apparent association constant (see Materials and Methods).

SEP proteins assemble into floral quartet-like complexes on CArG-boxes of direct target genes

In the above described experiments, self-tailored DNA-probes were used to study tetrameric complex assembly of the SEP proteins. To examine whether tetrameric complexes can also constitute on direct target genes of SEP proteins, DNA-binding to CArG-boxes in the regulatory regions of *AP3* and *SEP3* was analysed. The regions containing the CArG-boxes in these two target genes are evolutionarily conserved (Supplementary Figure S2) and have been shown to be of regulatory importance (15,29–30).

To study the binding of SEP proteins to *AP3*, a region spanning base pairs 220 to 123 upstream of the translation start site and carrying three CArG-boxes (termed CArG1, CArG2 and CArG3 here, with CArG3 being closest to the transcription start site; Figure 4) was used as a probe (Supplementary Table S2). This probe is termed *rAP3* (*r*egulatory region of *AP3*) henceforth. Also, derivatives of this probe were analysed in which one or two of the three CArG-boxes were mutated by substituting nucleotides C and G surrounding the A/T-rich CArG-box core with A's or T's (Supplementary Table S2). These derivatives were termed *rAP3m1* (CArG1 mutated); *rAP3m2* (CArG2 mutated); *rAP3m3* (CArG3 mutated); *rAP3m1,2* (CArG1 and

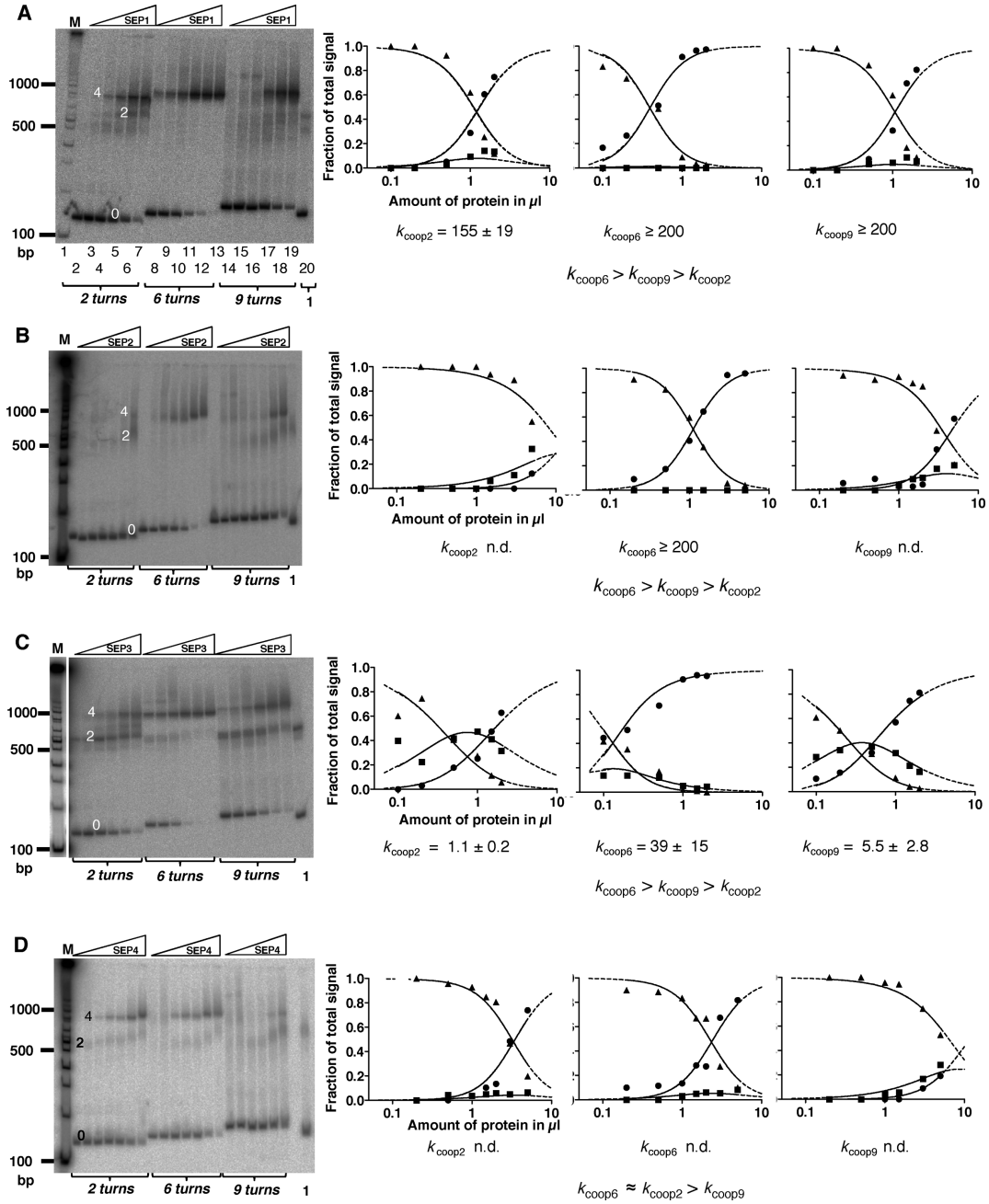

Figure 3. EMSAs to determine cooperativity of DNA binding by the four SEP proteins with DNA probes having CArG-boxes separated by 2, 6 or 9 helical turns. Increasing amounts of *in vitro* translated SEP proteins were titrated against a constant amount of DNA. The DNA probes used are denoted below the gels. The volumes of *in vitro* translated protein solution used for the binding reactions were (in µl): 0.1, 0.2, 0.5, 1.0, 1.5 and 2.0 for SEP1 (A), 0, 0.2, 0.5, 1.0, 1.5, 2.0 (only for the 9 turns probe), 3.0 and 5.0 for SEP2 (B), 0.1, 0.2, 0.5, 1.0, 1.5 and 2.0 for SEP3 (C), 0.2, 0.5, 1.0, 1.5, 2.0, 3.0 and 5.0 for SEP4 (D). In the right most lane of each gel, the respective protein was incubated with a DNA probe containing one CArG-box only for size comparison. Lane and band labelling is analogous to Figures 1 and 2. Quantitative analysis of the binding of individual proteins to the different probes is shown beside the respective gel. Fractional saturation is plotted as a function of the volume of *in vitro* translated protein solution (circles: two dimers or one tetramer bound; squares: one dimer bound; triangles: free DNA). Graphs were determined as described (18,24) with the broken lines indicating inferences below or above the protein amounts tested. k_{coop} values are shown below each graph ($n \geq 3$). Based on comparisons of band intensities of complexes comprising four proteins bound to DNA also k_{coop} comparisons are shown below the graphs. As described in Materials and Methods, k_{coop} values above 200 could not be resolved reliably. n.d., not determined. In these cases, the number of data points for which substantial protein binding was observed was too low to estimate k_{coop}.

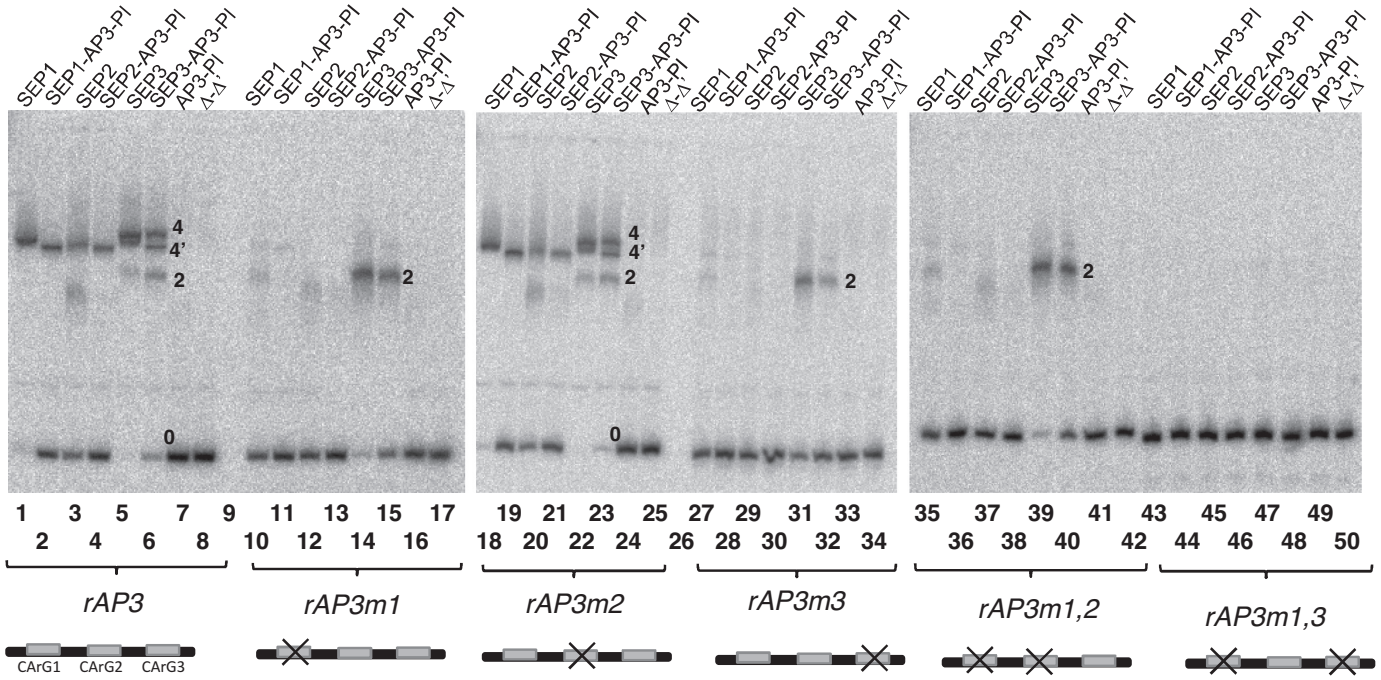

Figure 4. Binding of SEP proteins to CArG-boxes derived from the regulatory region of *AP3*. DNA probes used are denoted below the gel. The volume of *in vitro* translated protein solution used in the binding reaction was 2 μl. If more than one protein is denoted, co-translations were used. Lane and band labelling is analogous to Figure 1. Δ-Δ′ represents a negative control in which the *in vitro* translation assay was programmed by empty pTNT and pSPUTK vectors not containing a cDNA insert. 4′ represents a potential heterotetrameric protein-DNA complex.

CArG2 mutated) and *rAP3m1,3* (CArG1 and CArG3 mutated). Binding of SEP1 and SEP2 to *rAP3m1* and *rAP3m3* was very weak. In contrast, binding to the wild-type fragment *rAP3* as well as to *rAP3m2* resulted in the formation of easily detectable protein-DNA complexes (Figure 4, compare lanes 1, 3 and 18, 20 to lanes 10, 12 and 27, 29, for example). This indicates that SEP1 and SEP2 bound cooperatively to *rAP3*, and that CArG1 and CArG3, but not CArG2, are important for this cooperative binding.

As floral quartet-like complexes containing SEP, AP3 and PI are implicated in controlling petal development (12,31) and believed to activate *AP3*, we aimed to determine if complexes composed of SEP1, AP3 and PI or of SEP2, AP3 and PI could be reconstituted. In these experiments, AP3 and PI were always added together, as only the heterodimer is capable of binding to DNA (32) and forming DNA-bound tetramers with SEP3 (Supplementary Figure S4). Indeed, when AP3, PI and SEP1 or SEP2 were co-translated and incubated with *rAP3*, a protein-DNA complex of slightly higher mobility than that of the corresponding SEP1 or SEP2 homotetramer was detected (Figure 4, compare lanes 1 and 2 or 3 and 4, respectively), indicating that SEP1 or SEP2, AP3 and PI together bind to this DNA-probe. Such a complex was also detected with *rAP3m2*, but not or only very weakly with *rAP3m1* or *rAP3m3*, indicating that CArG1 and CArG3 are also critical for heterotetramer formation (Figure 4).

For SEP3, the binding pattern was slightly different. A complex migrating with an electrophoretic mobility similar to that of SEP1 and SEP2 homotetramers was detected with *rAP3* (Figure 4, lane 5); however, strong signals presumably representing individual dimers bound to CArG1 or CArG3 were obtained with *rAP3m1*, *rAP3m3* and *rAP3m1,2* (Figure 4, lanes 14, 31, 39). We were therefore not able to decide whether the complex formed on *rAP3* constitutes a SEP3 homotetramer or two dimers of SEP3 bound independently to CArG1 and CArG3. However, when SEP3 was co-translated with AP3 and PI, a novel complex binding to *rAP3* was detected. The electrophoretic mobility of this complex was slightly higher than that of the presumptive SEP3 homotetramer (Figure 4, compare lanes 5 and 6), indicating that a heterotetramer has been formed.

In principle, the slight mobility differences observed when SEP proteins alone and in combination with AP3/PI bound to *rAP3* may also be interpreted as independent binding of SEP homodimers and AP3/PI heterodimers to the DNA probe. The fact that AP3/PI heteromdimers have a lower molecular weight than SEP homodimers (51 kDa versus 57–59 kDa) and that AP3/PI may bend DNA differently as compared to SEP proteins and hence induce different DNA conformations is compatible with this view. However, AP3 and PI barely formed any protein-DNA complex on *rAP3* when no SEP protein was present (Figure 4, lane 7), suggesting that SEP proteins facilitate binding of AP3/PI to DNA, a fact that is most easily explained with the formation of heterotetrameric complexes.

In summary, SEP1, SEP2 and SEP3 can assemble with AP3 and PI into heterotetrameric complexes on the regulatory region of *AP3*.

We were not able to reproducibly detect binding of SEP4 to *rAP3* (Supplementary Figure S3). Very likely, this was due to the insufficient production of DNA-binding SEP4

protein (see Materials and Methods). However, a weak protein-DNA complex was observed when SEP4 was co-translated with AP3 and PI, indicating that SEP4 can at least constitute a heterotetrameric complex with AP3 and PI (Supplementary Figure S3).

We also analysed binding of individual SEP proteins alone and in combination with AP3 and PI to a highly conserved regulatory region of the *SEP3* gene that covered base pairs 3053 to 2931 upstream of the translation start, termed *rSEP3* here. This fragment contains two CArG-boxes (Supplementary Table S2) that have been shown to be bound by SEP3 *in vitro* and *in vivo* (15,33), suggesting that like *AP3*, also *SEP3* is under direct autoregulatory control.

Varying amounts of SEP3 were incubated with a constant amount of *rSEP3*. With low amounts of protein, protein-DNA complexes of intermediate mobility were resolved, indicative of a single dimer bound to either of the CArG-boxes (Figure 5, lanes 31 and 32). Using higher amounts of protein, complexes of lower electrophoretic mobility were also resolved (Figure 5, lanes 33 and 34). The two CArG-boxes on *rSEP3* have different sequences (Supplementary Figure S2B) and hence are probably bound with different affinities. It is therefore difficult to say whether the low-mobility complexes observed with high protein concentrations are formed cooperatively (24). In any case, the binding of SEP1 to *rSEP3* was markedly different from that of SEP3. For SEP1, individual DNA-bound dimers were barely detected; instead, only complexes of low electrophoretic mobility were observed (Figure 5, compare lanes 8, 9 with lanes 31 to 34). This indicates that SEP1 homotetramers bound cooperatively to *rSEP3*. We next assayed whether also heterotetrameric complexes composed of SEP1 or SEP3 and AP3/PI could be reconstituted on the *rSEP3* fragment. Low amounts of either SEP proteins or AP3/PI alone did not show any or only very limited binding to *rSEP3* (Figure 5). However, co-incubation of low amounts of SEP1 or SEP3 with increasing amounts of AP3/PI readily led to the formation of protein-DNA-complexes of low electrophoretic mobility, indicating that heterotetrameric complexes were formed with *rSEP3* (Figure 5, lanes 14–17 and 39–42). SEP2 barely showed any binding when assayed alone, but heterotetrameric complexes were observed when SEP2 was co-incubated with AP3/PI (Figure 5, lanes 18–21). Binding of SEP4 to *rSEP3* either alone or in combination with AP3/PI was very weak (Figure 5, lanes 43–46), thereby making inferences on cooperative binding of SEP4 to *rSEP3* impossible.

Cooperative binding decreases binding energy substantially

In our assays we determined binding of SEP proteins to 'naked' DNA. However, nucleosomal DNA present in the plant nucleus may impose considerable constraints on protein–DNA interactions. We therefore calculated protein concentrations necessary for half-saturating naked and nucleosomal DNA. Half-saturation is defined here as the protein dimer concentration at which 50% of the DNA fragments have both their CArG-boxes occupied by SEP dimers. We calculated the protein concentrations necessary to half-occupy both CArG-boxes simultaneously for DNA possessing inter-site distances of 2 or 6 helical turns using Equations (14) and (17). The equilibrium association constants $K_{\mathrm{dim}N,}$ determined for the binding of a single dimer to naked DNA (Table 1) and the k_{coop} values determined for the respective probes and proteins (Figure 3) were employed for the calculations. For the binding to naked DNA (Figure 6A), half-occupation was achieved at a protein dimer concentration of ≈1.5 nM when the proteins bound strongly cooperatively to the DNA (i.e. when CArG-boxes were separated by 6 helical turn for SEP1, SEP2 and SEP3 or by 2 turns for SEP1; Figure 6B and C, Supplementary Table S3). Binding of SEP3 to the DNA probe in which CArG-boxes were separated by 2 helical turns was barely cooperative. This was reflected in the ≈10-fold higher protein concentrations (15 nM) required for half-saturation.

We next calculated half saturation under the assumption that one of the two CArG-boxes is covered by histones (Figure 6A). Biophysical studies have shown that DNA rapidly unwraps and rewraps around the histone octamer, leading to transient accessibility of transcription factor binding sites (34–37). The energy penalty for accessing binding sites buried within nucleosomes is around 6.0–25.0 kJ/mol, depending on how deep within the nucleosome the binding site is located and hence how likely the binding site is exposed by unwrapping and rewrapping (34–35,38). To estimate the protein concentrations necessary for half-occupation in a nucleosomal context, an energy penalty of 20.92 kJ/mol (5 kcal/mol) was introduced. In this case, half occupation was achieved at a dimer concentration of ≈1000 nM when binding was cooperative (Figure 6B and C). This concentration corresponds to ≈42 000 SEP dimers per nucleus when a nuclear volume of 70 μm^3 (39) is assumed. However, when binding of two dimers was largely non-cooperative (binding of two SEP3 dimers to CArG-boxes separated by 2 helical turns), half saturation was calculated to be achieved only at very high protein dimer concentrations of 60 600 nM (Figure 6B and C), which would correspond to ≈2 500 000 SEP3 protein dimers per nucleus.

DISCUSSION

The SEP proteins have distinct DNA-binding properties

Our protein-DNA interaction analyses indicate that the four SEP proteins assemble on DNA in a largely similar manner. All of them constitute tetrameric complexes by cooperatively binding to DNA fragments carrying CArG-boxes separated by only a few helical turns. Also, the degree of cooperative binding dropped for inter-site distances below or above the optimal CArG-box spacing. Interestingly, *in vivo* binding analyses of SEP3 by ChIP-Seq studies showed an enrichment of CArG-box pairs separated by 4 helical turns (33). This is consistent with our results where high amounts of tetrameric SEP3 complexes were observed when the CArG-boxes were separated by 4, 5 or 6 helical turns (Figure 3). Thus, the inherent inter-site distance preferences for cooperative DNA-binding determined here may be a major factor in determining *in vivo* target gene specificity.

The inter-site distances for which cooperative DNA-binding was detected were 63 bp or below and thus well below the persistence length of DNA (about 150 bp). Bending of DNA shorter than the persistence length was long

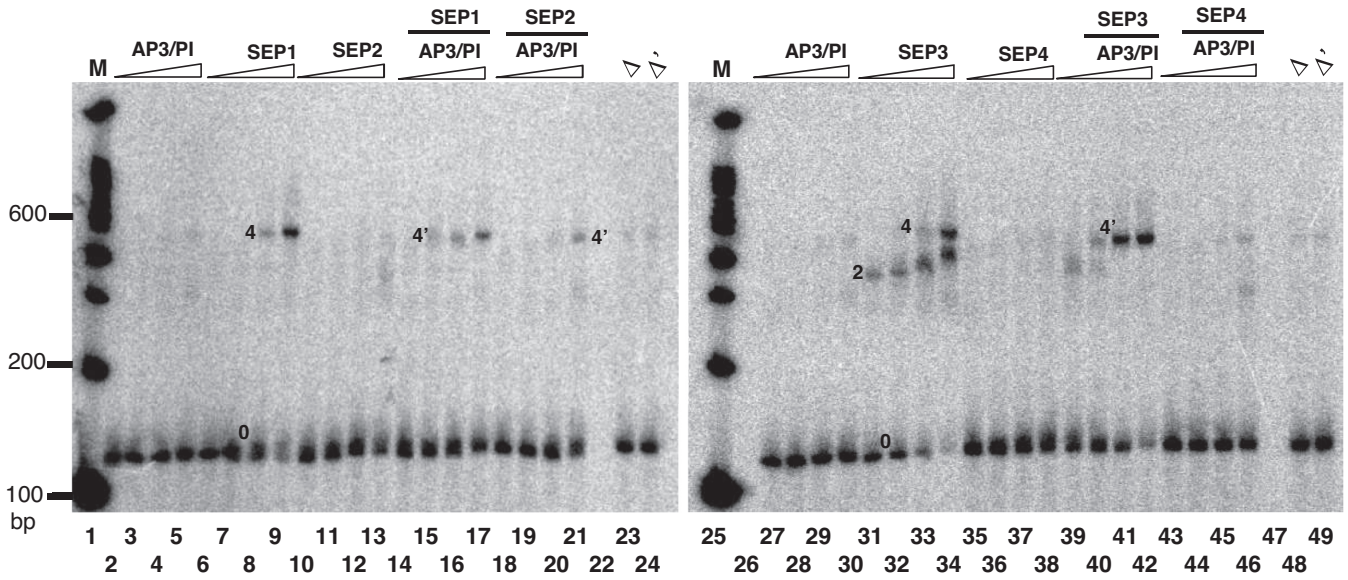

Figure 5. Binding of SEP proteins to CArG-boxes derived from the regulatory region of *SEP3*. The proteins used are denoted above the gel. The increasing volumes of *in vitro* translated protein solution used in the binding reactions were 0.2, 0.5, 1.5 and 4.0 μl each. In case of mixing SEP with AP3 and PI, 0.2 μl of the respective SEP protein solution was mixed with increasing volumes (0.2, 0.5, 1.5 and 4 μl) of *in vitro* translation solutions containing AP3 and PI. Lane and band labelling is analogous to Figures 1 and 2. Δ and Δ′ represents a negative control in which the *in vitro* translation assay was programmed only by pTNT and pSPUTK vectors, respectively, not containing a cDNA insert. 4′ represents a potential heterotetrameric protein-DNA complex.

assumed to be energetically highly unfavourable (40). However, recent experimental evidence indicates that DNA flexibility over distances below the persistence length is way more common than has been previously anticipated (41–43). Thus, the proposed SEP protein-induced DNA-looping and tetramer formation over short inter-site distances may require only a limited amount of interaction energy between the DNA-bound dimers. The hypothesis that protein-induced DNA-loops are possible over these short distances is further supported by the fact that the phage λ repressor and the lac repressor—both paradigms for protein–DNA interactions—are capable of looping DNA over similarly short distances (44,45).

Very likely, the ability to cooperatively bind to DNA is of prime importance for SEP proteins to function as developmental switches during flower formation (20). The similarity in the cooperative binding behaviour may therefore at least partly explain why the different SEP proteins function redundantly to a large extent during flower development. Interestingly, SEP3, which showed the least cooperative binding to CArG-boxes separated by 6 helical turns, showed the strongest inherent affinity to an individual CArG-box (Table 1). Thus, low cooperative binding may, at appropriate targets, at least partly be compensated for by high affinity of protein dimers to individual CArG-boxes.

However, despite overall similarities, it is evident that each of the SEP proteins possesses characteristic DNA-binding properties. For example, in our experiments SEP1 bound strongly cooperatively to CArG-box pairs separated by small as well as large distances whereas for SEP2 and SEP4 strong cooperative binding was detected only for large or small distances, respectively (Figures 2 and 3). For SEP3, cooperative binding was comparatively weak for most of the inter-site distances tested (Figure 3). Differences in cooperative DNA-binding persisted when regulatory regions of SEP proteins' target genes were analysed. For example, SEP1 appeared to bind with higher cooperativity to *rSEP3* than SEP3. These differences in cooperative binding behaviour may allow for an intricate regulation of different sets of target genes, thereby accounting for different functions performed by the individual SEP proteins.

We detected homo- as well as heterotetramer formation of the different SEP proteins. Ectopic expression of SEP proteins together with AP3 and PI leads to the development of petaloid organs from primordia that normally develop leaves (12,31). This indicates that a SEP/SEP-AP3/PI heterotetramer is involved in petal specification (12,21). Though AP1 is also important for determining petal identity, and was proposed to be part of the respective tetrameric complex (19,46), there is also evidence that this protein is not strictly required for petal development (see 21,47 for a more comprehensive discussion on that subject). The developmental role of SEP homotetramers remains unclear (18). Indeed, the data presented here support previous notions that heterotetramer formation of SEP proteins with other partners may in many cases be favoured over homotetramer formation (15,21,48). However, while *SEP* genes are expressed at stage 2 of flower development (3,8,10–11), the expression of their potential interaction partners AP3, PI or AG is only detected from stage 3 onwards (49–51). This raises the possibility that SEP proteins form homotetramers at least during early stages of flower development when appropriate partners for heterotetramer formation are absent (18). Additionally, SEP3 especially has been shown to have a prominent role in activating AP3, PI and AG (7), supporting the hypothesis that individual SEP homotetramers possess divergent functions during flower development. However, it can presently also not be excluded that SEP pro-

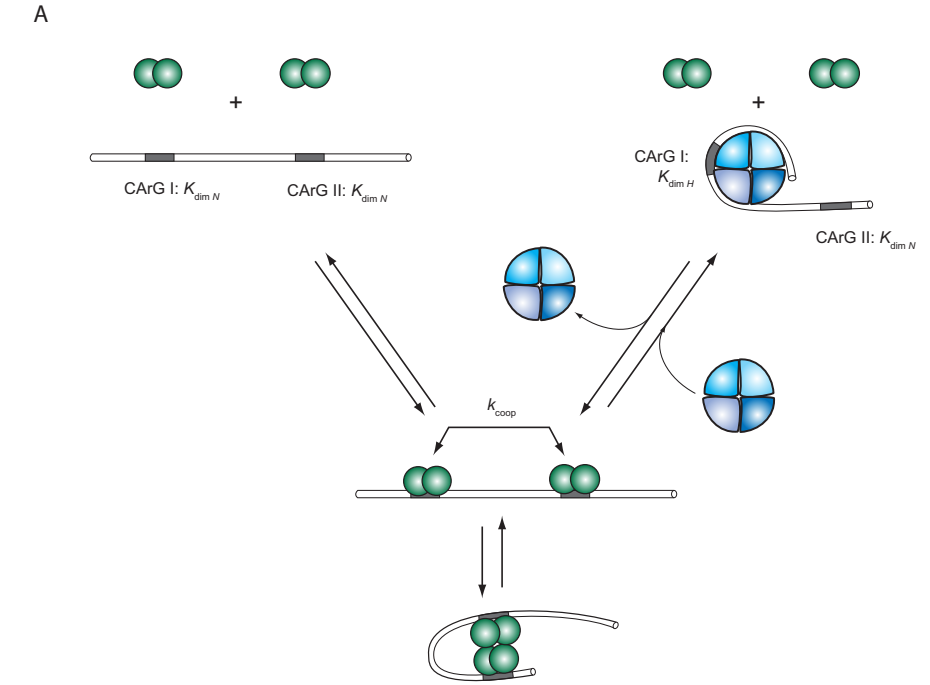

B

	Protein concentration necessary to half-occupy both CArG-boxes simultaneously (nM)			
	Naked DNA		Nucleosomal DNA	
	CArG I and II spaced by 2 turns	CArG I and II spaced by 6 turns	CArG I and II spaced by 2 turns	CArG I and II spaced by 6 turns
SEP1	1.7	≤ 1.5	1,300	≤ 1000
SEP2	n.d.	≤ 1.1	n.d.	≤ 750
SEP3	15	1.3	60,600	1,700

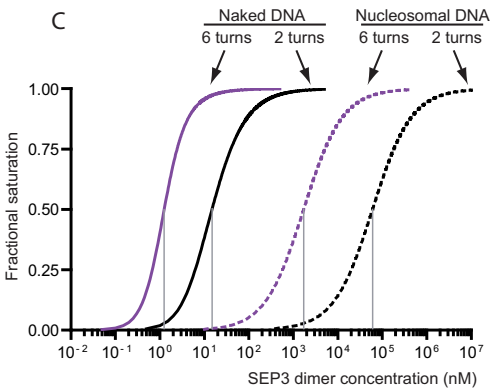

Figure 6. Model for binding of SEP proteins to naked and nucleosomal DNA. (A) Proposed mechanism for DNA-binding and potential complex formation of two SEP protein dimers (green circles). Binding to naked DNA (left) and to DNA partly wrapped on histones (right; histones shown in blue) is depicted. Binding of a dimer to a CArG-box not covered by histones is characterized by the affinity constant $K_{\mathrm{dim}N}$, binding to a histone-covered CArG-box is described by $K_{\mathrm{dim}H}$. Cooperative interactions are described by k_{coop}. The histones are displaced completely from the DNA here for simplicity. However, partial unwrapping resulting in exposure of the CArG-box may suffice for SEP protein binding. (B) SEP protein concentrations required for half-saturation of DNA with CArG-boxes spaced by 2 or 6 helical turns. See Supplementary Table S3 for a comprehensive overview over all values used for the calculations. (C) Simulated transition curves for simultaneous binding of two SEP3 dimers to CArG-boxes separated by 2 (black lines) and 6 (lilac line) helical turns. Binding to naked (solid lines) or nucleosomal (dotted lines) DNA is plotted. K_{dim} and k_{coop} values from Table 1 and Figure 3 have been used to calculate the transition curves with Equations (14) and (17). Grey vertical lines indicate protein concentrations at which half-occupation (i.e. fractional saturation = 0.5) is achieved.

teins interact with other MADS-domain transcription factors like AP1 early during flower development to activate AP3, PI and AG (52). These uncertainties notwithstanding it is plausible to assume that the inherent differences in DNA-binding among the individual SEP protein homotetramers will at least to some extent also be relevant for heterotetramer formation and thereby target gene regulation by heterotetramers, and are therefore of considerable scientific interest.

The differences in DNA-binding among the individual SEP proteins may be one reason for the phenotypic differences observed between some triple mutants. While *sep1 sep2 sep3* plants show strong defects with all floral organs being transformed into sepals, *sep1 sep2 sep4* plants have been described to be phenotypically normal (2,3). Our data show that SEP4 binds cooperatively only to a restricted range of CArG-box distances. The protein may therefore not be able to regulate the entire set of target genes required for floral organ development. This is in contrast to SEP3, which, at a given protein concentration shows binding to a larger range of distances between the CArG-boxes (Figure 2) and thus presumably to a wider spectrum of target genes. This may partly explain why SEP3 but not SEP4 is able to govern floral organ development in the absence

of SEP1 and SEP2 (2,3). It should be kept in mind, however, that other differences between the SEP proteins like distinct spatio-temporal expression patterns and expression strengths very likely also contribute to differences in SEP functions.

Differential cooperative binding abilities could also be responsible for the differential sensitivity of SEP proteins to variations in gene dosage. *SEP1/sep1 sep2 sep3* plants and also *sep1 SEP2/sep2 sep3* plants, but not *sep1 sep2 SEP3/sep3* plants show defects in ovule development (53). Cooperative binding affinity to certain inter-site distances was stronger for SEP1 and SEP2 than for SEP3 (Figure 3). Such a strong cooperativity in DNA-binding may create a switch-like occupancy of target genes, thereby rendering DNA-binding by SEP1 and SEP2 more susceptible to variations in protein concentration than DNA-binding of SEP3 (if concentration is varied in a range critical for the switch-like occupancy of target genes). If gene dosage and protein concentration are positively correlated, as seems plausible, differences in cooperative binding abilities may lead to an increased dosage sensitivity of SEP1 and SEP2 as compared to SEP3.

Floral quartets assemble on regulatory regions of target genes

Notably, SEP proteins formed heterotetrameric complexes with AP3/PI on the regulatory regions of the target genes *SEP3* and *AP3*. Also, these heterotetramers formed more readily than homotetramers (Figures 4 and 5), confirming and extending previous observations made with complexes composed of SEP3 and other floral homeotic proteins (15,21,48). Intriguingly, cooperative DNA-binding to *rAP3* required CArG1 and CArG3, but not CArG2. CArG1 and CArG3 are separated by ≈7 helical turns, whereas the inter-site distance between CArG1 and CArG2 or CArG2 and CArG3 corresponds to 4.6 and 2.4 helical turns, respectively. Probes with an inter-site distance of 7 helical turns are strongly bound by SEP1, SEP2 and SEP3 but not by SEP4, which may partly explain the differential complex formation properties on *rAP3*. It should be kept in mind, however, that the binding strength of dimers to the individual CArG-boxes also contributes to the overall binding affinity. For example, in contrast to CArG1 and CArG3, CArG2 is barely bound, if at all, by MADS-domain protein dimers (29,30), thus offering an additional explanation for the dispensability of CArG2 for tetramer formation.

Cooperative binding to *rSEP3* was observed although the CArG-boxes were separated ≈5.4 helical turns from each other. Though cooperativity would be expected to be stronger if CArG-boxes are separated by full helical turns it might still be possible to achieve cooperativity if binding sites are separated by a non-integral number of turns. Factors that play a role here are the interaction strength between the two dimers, the flexibility of the proteins and the DNA and the looping geometry. For example, it has been demonstrated previously for the lac repressor that alternative looping geometries can also confer binding to non-integrally spaced binding sites (54).

Our data support the idea that tetramer formation is a dynamic process and that differential tetramer binding affinity may be one mechanism responsible for differential target gene regulation (21,47). For example, early in development SEP homotetramers may form and target a restricted set of genes that function in floral meristem specification. Later, complexes composed of SEP, AP3 and PI may form that possess a higher DNA-binding affinity as compared to SEP homotetramers, thereby also regulating genes that are not targeted by SEP proteins alone (21). It remains to be determined to which extent the complex formation of SEP proteins with floral meristem identity proteins like AP1 or flowering time proteins like AGAMOUS-LIKE 24 (AGL24) or SHORT VEGETATIVE PHASE (SVP) (14) is compatible with this model.

Protein concentration and the formation of floral quartets

Our study indicates that tetramerization of SEP proteins strongly depends on the distance between and orientation of the two CArG-boxes to each other. For example, from our calculations, ≈10 times the amount of SEP3 protein is needed to achieve half-occupancy of CArG-boxes separated by 2 helical turns of DNA as compared to CArG-boxes separated by 6 turns, if binding to naked DNA is considered (Figure 6B and C). This may have profound influences on the dynamics of target gene regulation *in vivo*. Furthermore, the sequence of the DNA between the CArG-boxes may influence looping propensensity; if the region between the CArG-boxes possesses an intrinsic curvature looping may be facilitated in comparison to 'straight' DNA (55). The affinity of a given SEP protein dimer for individual CArG-boxes may also vary (16–17,55), thereby introducing another layer of complexity. Finally, various combinations of CArG-box sequences, distances and orientations may constitute different *cis*-regulatory modules, which could be occupied by SEP proteins at specific protein concentrations. Concentration-dependent target gene regulation is well known from a number of systems, one paradigmatic example being the regulation of zygotic genes by maternal effect genes during *Drosophila* development (56). Whether variations in SEP protein concentration during development are responsible for differential target gene regulation has not been demonstrated so far. However, gene dosage experiments indicate that differences in protein concentrations may play a role. As mentioned above, inactivation of one SEP1 allele in a *sep2 sep3* double mutant background leads to severe abnormalities in ovule development in otherwise normal flowers (53). A further reduction of SEP1 activity by creating a *sep1 sep2 sep3* triple mutant results in flowers consisting of sepals only (2). This may be taken as evidence that high concentrations of SEP proteins are necessary for ovule development and that lower concentrations suffice for the development of the floral organs. Consistent with this conclusion, ectopic expression of SEP3 occasionally leads to the formation of ovules on first-whorl sepals (47).

Clearly, however, more systematic and quantitative studies on the influence of protein levels on target gene expression have to be carried out to reveal whether variations in protein concentration are employed to regulate different target genes in different tissues and thus to generate complex floral organs.

Floral quartet formation and chromatin state

Our affinity estimates for the binding of two SEP dimers to DNA indicate that protein concentrations necessary to half-occupy binding sites are very low for naked DNA, but might be considerably higher for nucleosomal DNA (Figure 6B and C). Importantly, protein concentrations necessary for half-occupation of nucleosomal DNA strongly depended on the ability of SEP dimers to cooperatively interact with each other. For example, while SEP3 concentrations necessary for half-saturation of non-cooperatively versus cooperatively bound CArG-box pairs (i.e. inter-site distances of 2 turns versus 6 turns) differed ≈10-fold when naked DNA was considered, concentration differences of more than 30-fold were inferred for nucleosomal DNA (Figure 6B and C). Thus, the degree of cooperative DNA-binding may well contribute to differential target gene binding especially in a nucleosomal context.

Abundance of individual transcription factors is usually within the range of 250 molecules to 300 000 molecules per nucleus (57–60). Although the number of SEP molecules in a plant nucleus is not known, it is feasible to assume that it falls into this range. According to our calculations, a very high SEP3 dimer abundance of 2 500 000 molecules per nucleus would be necessary to half-occupy nucleosomal DNA if binding is non-cooperative. Non-cooperatively binding SEP dimers may thus barely be able to bind histone-associated DNA. In contrast, taking cooperative DNA-binding and tetramer formation into account, comparatively moderate SEP amounts of around 42 000 molecules per nucleus may suffice to half-occupy binding sites in a nucleosomal context (Figure 6). It was recently demonstrated that SEP3 binds to enhancer sites very early during flower development and that chromatin accessibility changes only subsequently (61). It was thus proposed that SEP3 acts as a pioneer factor that modifies chromatin accessibility (61). Even though our calculations are only rough estimates and the true figures may vary substantially depending on the sequence of the CArG-boxes, the inter-site distance between CArG-boxes and chromatin modifications, they nevertheless indicate that the ability of cooperative DNA-binding of SEP proteins is of critical importance to invade nucleosomal DNA and hence to act as pioneer factors.

It is interesting to note that transcription factors can in principle cooperatively assemble on nucleosomal DNA even if they do not directly interact with each other (35,62). This is attained because transcription factors binding in vicinity to each other may 'share' the energy penalty required to displace histones from DNA (35,62). Histones are most effectively displaced by DNA-binding proteins whose binding sites are spaced by up to 74 bp from each other (35,62), a distance that is close to the CArG-box distances for which highest cooperativity was observed in this study.

In conclusion, it remains an important goal for future research to untangle the dynamic composition of tetrameric MADS-domain protein complexes during flower development and to further unravel the relevance of the CArG-box sequences, the inter-site distance between the CArG-boxes, the stereo-specific orientation of the CArG-boxes, the chromatin state and the binding differences among MADS-domain proteins to approach at a detailed understanding of how target gene specificity is determined.

SUPPLEMENTARY DATA

Supplementary Data are available at NAR Online.

ACKNOWLEDGEMENTS

We are grateful to Christian Gafert for excellent technical support and to Lydia Gramzow for help with the retrieval of *SEP3* and *AP3* regulatory regions from diverse Brassicaceae species. We thank five anonymous reviewers for helpful comments on an earlier version of this manuscript. R.M. thanks the University of Leipzig for general support. We thank Matthias Brock (HKI Jena) for helpful discussions.

FUNDING

Fellowship from the International Leibniz Research School for Microbial and Biomolecular Interactions (ILRS Jena) [to K.J.], which is part of the Jena School for Microbial Communication (JSMC). Fellowship from the Carl-Zeiss-Stiftung [to R.M.]. Source of open access funding: Carl-Zeiss-Stiftung.
Conflict of interest statement. None declared.

REFERENCES

1. Smaczniak,C., Immink,R.G., Angenent,G.C. and Kaufmann,K. (2012) Developmental and evolutionary diversity of plant MADS-domain factors: insights from recent studies. *Development*, **139**, 3081–3098.
2. Pelaz,S., Ditta,G.S., Baumann,E., Wisman,E. and Yanofsky,M.F. (2000) B and C floral organ identity functions require SEPALLATA MADS-box genes. *Nature*, **405**, 200–203.
3. Ditta,G., Pinyopich,A., Robles,P., Pelaz,S. and Yanofsky,M.F. (2004) The SEP4 gene of Arabidopsis thaliana functions in floral organ and meristem identity. *Curr. Biol.*, **14**, 1935–1940.
4. Zahn,L.M., King,H.Z., Leebens-Mack,J.H., Kim,S., Soltis,P.S., Landherr,L.L., Soltis,D.E., dePamphilis,C.W. and Ma,H. (2005) The evolution of the *SEPALLATA* subfamily of MADS-box genes: a preangiosperm origin with multiple duplications throughout angiosperm history. *Genetics*, **169**, 2209–2223.
5. Jack,T. (2001) Relearning our ABCs: new twists on an old model. *Trends Plant Sci.*, **6**, 310–316.
6. Pelaz,S., Gustafson-Brown,C., Kohalmi,S.E., Crosby,W.L. and Yanofsky,M.F. (2001) APETALA1 and SEPALLATA3 interact to promote flower development. *Plant J.*, **26**, 385–394.
7. Liu,C., Xi,W., Shen,L., Tan,C. and Yu,H. (2009) Regulation of floral patterning by flowering time genes. *Dev. Cell*, **16**, 711–722.
8. Mandel,M.A. and Yanofsky,M.F. (1998) The Arabidopsis AGL9 MADS box gene is expressed in young flower primordia. *Sex Plant Reprod.*, **11**, 22–28.
9. Ma,H., Yanofsky,M.F. and Meyerowitz,E.M. (1991) *AGL1-AGL6*, an *Arabidopsis* gene family with similarity to floral homeotic and transcription factor genes. *Gene Dev.*, **5**, 484–495.
10. Flanagan,C.A. and Ma,H. (1994) Spatially and temporally regulated expression of the MADS-box gene AGL2 in wild-type and mutant Arabidopsis flowers. *Plant Mol. Biol.*, **26**, 581–595.
11. Savidge,B., Rounsley,S.D. and Yanofsky,M.F. (1995) Temporal relationship between the transcription of 2 Arabidopsis MADS-box genes and the floral organ identity genes. *Plant Cell*, **7**, 721–733.
12. Honma,T. and Goto,K. (2001) Complexes of MADS-box proteins are sufficient to convert leaves into floral organs. *Nature*, **409**, 525–529.
13. de Folter,S., Immink,R.G.H., Kieffer,M., Parenicova,L., Henz,S.R., Weigel,D., Busscher,M., Kooiker,M., Colombo,L., Kater,M.M. *et al.* (2005) Comprehensive interaction map of the *Arabidopsis* MADS box transcription factors. *Plant Cell*, **17**, 1424–1433.

14. Immink,R.G., Tonaco,I.A., de Folter,S., Shchennikova,A., van Dijk,A.D., Busscher-Lange,J., Borst,J.W. and Angenent,G.C. (2009) SEPALLATA3: the 'glue' for MADS box transcription factor complex formation. *Genome Biol.*, **10**, R24.
15. Smaczniak,C., Immink,R.G., Muino,J.M., Blanvillain,R., Busscher,M., Busscher-Lange,J., Dinh,Q.D., Liu,S., Westphal,A.H., Boeren,S. *et al.* (2012) Characterization of MADS-domain transcription factor complexes in Arabidopsis flower development. *Proc. Natl. Acad. Sci. U.S.A.*, **109**, 1560–1565.
16. Huang,H., Tudor,M., Weiss,C.A., Hu,Y. and Ma,H. (1995) The *Arabidopsis* MADS-box gene AGL3 Is widely expressed and encodes a sequence-specific DNA-binding protein. *Plant Mol. Biol.*, **28**, 549–567.
17. Huang,H., Tudor,M., Su,T., Zhang,Y., Hu,Y. and Ma,H. (1996) DNA binding properties of two *Arabidopsis* MADS domain proteins: binding consensus and dimer formation. *Plant Cell*, **8**, 81–94.
18. Melzer,R., Verelst,W. and Theissen,G. (2009) The class E floral homeotic protein SEPALLATA3 is sufficient to loop DNA in 'floral quartet'-like complexes in vitro. *Nucleic Acids Res.*, **37**, 144–157.
19. Theißen,G. (2001) Development of floral organ identity: stories from the MADS house. *Curr. Opin. Plant Biol.*, **4**, 75–85.
20. Theißen,G. and Melzer,R. (2007) Molecular mechanisms underlying origin and diversification of the angiosperm flower. *Ann. Bot-London*, **100**, 603–619.
21. Melzer,R. and Theissen,G. (2009) Reconstitution of 'floral quartets' in vitro involving class B and class E floral homeotic proteins. *Nucleic Acids Res.*, **37**, 2723–2736.
22. Riechmann,J.L., Wang,M.Q. and Meyerowitz,E.M. (1996) DNA-binding properties of *Arabidopsis* MADS domain homeotic proteins APETALA1, APETALA3, PISTILLATA and AGAMOUS. *Nucleic Acids Res.*, **24**, 3134–3141.
23. Man,T.K. and Stormo,G.D. (2001) Non-independence of Mnt repressor-operator interaction determined by a new quantitative multiple fluorescence relative affinity (QuMFRA) assay. *Nucleic Acids Res.*, **29**, 2471–2478.
24. Senear,D.F. and Brenowitz,M. (1991) Determination of binding constants for cooperative site-specific protein-DNA interactions using the gel mobility-shift assay. *J. Biol. Chem.*, **266**, 13661–13671.
25. Senear,D.F., Dalma-Weiszhausz,D.D. and Brenowitz,M. (1993) Effects of anomalous migration and DNA to protein ratios on resolution of equilibrium constants from gel mobility-shift assays. *Electrophoresis*, **14**, 704–712.
26. Tsai,S.Y., Tsai,M.J. and O'Malley,B.W. (1989) Cooperative binding of steroid hormone receptors contributes to transcriptional synergism at target enhancer elements. *Cell*, **57**, 443–448.
27. Kyas,A., Mäueler,W. and Epplen,J.T. (1998) Polyacrylamide gel electrophoresis of DNA/protein complexes. In: Tietz,D (ed). *Nucleic Acid Electrophoresis*. Springer, Berlin, Heidelberg, pp. 292–310.
28. Cao,Z.D., Umek,R.M. and Mcknight,S.L. (1991) Regulated expression of 3 C/Ebp isoforms during adipose conversion of 3t3-L1 cells. *Gene Dev.*, **5**, 1538–1552.
29. Hill,T.A., Day,C.D., Zondlo,S.C., Thackeray,A.G. and Irish,V.F. (1998) Discrete spatial and temporal cis-acting elements regulate transcription of the Arabidopsis floral homeotic gene APETALA3. *Development*, **125**, 1711–1721.
30. Tilly,J.J., Allen,D.W. and Jack,T. (1998) The CArG boxes in the promoter of the Arabidopsis floral organ identity gene APETALA3 mediate diverse regulatory effects. *Development*, **125**, 1647–1657.
31. Pelaz,S., Tapia-Lopez,R., Alvarez-Buylla,E.R. and Yanofsky,M.F. (2001) Conversion of leaves into petals in Arabidopsis. *Curr. Biol.*, **11**, 182–184.
32. Riechmann,J.L., Krizek,B.A. and Meyerowitz,E.M. (1996) Dimerization specificity of *Arabidopsis* MADS domain homeotic proteins APETALA1, APETALA3, PISTILLATA, and AGAMOUS. *Proc. Natl. Acad. Sci. U.S.A.*, **93**, 4793–4798.
33. Kaufmann,K., Muino,J.M., Jauregui,R., Airoldi,C.A., Smaczniak,C., Krajewski,P. and Angenent,G.C. (2009) Target genes of the MADS transcription factor SEPALLATA3: integration of developmental and hormonal pathways in the Arabidopsis flower. *PLoS Biol.*, **7**, e1000090.
34. Polach,K.J. and Widom,J. (1995) Mechanism of protein access to specific DNA sequences in chromatin: a dynamic equilibrium model for gene regulation. *J. Mol. Biol.*, **254**, 130–149.
35. Polach,K.J. and Widom,J. (1996) A model for the cooperative binding of eukaryotic regulatory proteins to nucleosomal target sites. *J. Mol. Biol.*, **258**, 800–812.
36. Li,G. and Widom,J. (2004) Nucleosomes facilitate their own invasion. *Nat. Struct. Mol. Biol.*, **11**, 763–769.
37. Li,G., Levitus,M., Bustamante,C. and Widom,J. (2005) Rapid spontaneous accessibility of nucleosomal DNA. *Nat. Struct. Mol. Biol.*, **12**, 46–53.
38. Tims,H.S., Gurunathan,K., Levitus,M. and Widom,J. (2011) Dynamics of nucleosome invasion by DNA binding proteins. *J. Mol. Biol.*, **411**, 430–448.
39. Dittmer,T.A., Stacey,N.J., Sugimoto-Shirasu,K. and Richards,E.J. (2007) LITTLE NUCLEI genes affecting nuclear morphology in Arabidopsis thaliana. *Plant Cell*, **19**, 2793–2803.
40. Nelson,P.C. (2012) Spare the (Elastic) Rod. *Science*, **337**, 1045–1046.
41. Cloutier,T.E. and Widom,J. (2004) Spontaneous sharp bending of double-stranded DNA. *Mol. Cell*, **14**, 355–362.
42. Cloutier,T.E. and Widom,J. (2005) DNA twisting flexibility and the formation of sharply looped protein-DNA complexes. *Proc. Natl. Acad. Sci. U.S.A.*, **102**, 3645–3650.
43. Vafabakhsh,R. and Ha,T. (2012) Extreme bendability of DNA less than 100 base pairs long revealed by single-molecule cyclization. *Science*, **337**, 1097–1101.
44. Hochschild,A. and Ptashne,M. (1986) Cooperative binding of lambda repressors to sites separated by integral turns of the DNA helix. *Cell*, **44**, 681–687.
45. Krämer,H., Niemoller,M., Amouyal,M., Revet,B., von Wilcken-Bergmann,B. and Müller-Hill,B. (1987) lac repressor forms loops with linear DNA carrying two suitably spaced lac operators. *EMBO J.*, **6**, 1481–1491.
46. Theißen,G. and Saedler,H. (2001) Plant biology. Floral quartets. *Nature*, **409**, 469–471.
47. Castillejo,C., Romera-Branchat,M. and Pelaz,S. (2005) A new role of the Arabidopsis SEPALLATA3 gene revealed by its constitutive expression. *Plant J.*, **43**, 586–596.
48. Mendes,M.A., Guerra,R.F., Berns,M.C., Manzo,C., Masiero,S., Finzi,L., Kater,M.M. and Colombo,L. (2013) MADS domain transcription factors mediate short-range DNA looping that is sssential for target gene expression in Arabidopsis. *Plant Cell*, **25**, 2560–2572.
49. Jack,T., Brockman,L.L. and Meyerowitz,E.M. (1992) The homeotic gene APETALA3 of Arabidopsis thaliana encodes a MADS box and is expressed in petals and stamens. *Cell*, **68**, 683–697.
50. Goto,K. and Meyerowitz,E.M. (1994) Function and regulation of the *Arabidopsis* floral homeotic gene *PISTILLATA*. *Gene Dev.*, **8**, 1548–1560.
51. Drews,G.N., Bowman,J.L. and Meyerowitz,E.M. (1991) Negative regulation of the Arabidopsis homeotic gene AGAMOUS by the APETALA2 product. *Cell*, **65**, 991–1002.
52. Gregis,V., Sessa,A., Dorca-Fornell,C. and Kater,M.M. (2009) The *Arabidopsis* floral meristem identity genes *AP1*, *AGL24* and *SVP* directly repress class B and C floral homeotic genes. *Plant J.*, **60**, 626–637.
53. Favaro,R., Pinyopich,A., Battaglia,R., Kooiker,M., Borghi,L., Ditta,G., Yanofsky,M.F., Kater,M.M. and Colombo,L. (2003) MADS-box protein complexes control carpel and ovule development in Arabidopsis. *Plant Cell*, **15**, 2603–2611.
54. Wong,O.K., Guthold,M., Erie,D.A. and Gelles,J. (2008) Interconvertible lac repressor-DNA loops revealed by single-molecule experiments. *Plos Biol.*, **6**, 2028–2042.
55. Muino,J.M., Smaczniak,C., Angenent,G.C., Kaufmann,K. and van Dijk,A.D.J. (2014) Structural determinants of DNA recognition by plant MADS-domain transcription factors. *Nucleic Acids Res.*, **42**, 2138–2146.
56. Lander,A.D. (2007) Morpheus unbound: reimagining the morphogen gradient. *Cell*, **128**, 245–256.
57. Biggin,M.D. (2011) Animal transcription networks as highly connected, quantitative continua. *Dev. Cell*, **21**, 611–626.
58. Gregor,T., Tank,D.W., Wieschaus,E.F. and Bialek,W. (2007) Probing the limits to positional information. *Cell*, **130**, 153–164.
59. Bolouri,H. and Davidson,E.H. (2003) Transcriptional regulatory cascades in development: initial rates, not steady state, determine network kinetics. *Proc. Natl. Acad. Sci. U.S.A.*, **100**, 9371–9376.

60. Simicevic,J., Schmid,A.W., Gilardoni,P.A., Zoller,B., Raghav,S.K., Krier,I., Gubelmann,C., Lisacek,F., Naef,F., Moniatte,M. *et al.* (2013) Absolute quantification of transcription factors during cellular differentiation using multiplexed targeted proteomics. *Nat. Methods*, **10**, 570–576.
61. Pajoro,A., Madrigal,P., Muino,J.M., Matus,J.T., Jin,J., Mecchia,M.A., Debernardi,J.M., Palatnik,J.F., Balazadeh,S., Arif,M. *et al.* (2014) Dynamics of chromatin accessibility and gene regulation by MADS-domain transcription factors in flower development. *Genome Biol.*, **15**, R41.
62. Moyle-Heyrman,G., Tims,H.S. and Widom,J. (2011) Structural constraints in collaborative competition of transcription factors against the nucleosome. *J. Mol. Biol.*, **412**, 634–646.